Stretch-induced Programmed Myocyte Cell Death

Wei Cheng,* Baosheng Li,* Jan Kajstura,* Peng Li,* Michael S. Wolin,‡ Edmund H. Sonnenblick,*§ Thomas H. Hintze,‡ Giorgio Olivetti,* and Piero Anversa*§

*Departments of *Medicine and ‡Physiology, New York Medical College, Valhalla, New York 10595; and §Department of Medicine, Albert Einstein College of Medicine, New York 10461*

Abstract

To determine the effects of loading on active and passive tensions, programmed cell death, superoxide anion formation, the expression of Fas on myocytes, and side-to-side slippage of myocytes, papillary muscles were exposed to 7–8 and 50 mN/mm^2 and these parameters were measured over a 3-h period. Overstretching produced a 21- and a 2.4-fold increase in apoptotic myocyte and nonmyocyte cell death, respectively. Concurrently, the generation of reactive oxygen species increased 2.4-fold and the number of myocytes labeled by Fas protein 21-fold. Moreover, a 15% decrease in the number of myocytes included in the thickness of the papillary muscle was found in combination with a 7% decrease in sarcomere length and the inability of muscles to maintain stable levels of passive and active tensions. The addition of the NO-releasing drug, C87-3754, prevented superoxide anion formation, programmed cell death, and the alterations in active and passive tensions with time of overloaded papillary muscles. In conclusion, overstretching appears to be coupled with oxidant stress, expression of Fas, programmed cell death, architectural rearrangement of myocytes, and impairment in force development of the myocardium. (*J. Clin. Invest.* 1995. 96:2247–2259.) Key words: biotinylated dUTP labeling • apoptosis • overstretching • Fas protein • morphometry • reactive oxygen species

Introduction

Recently, the possibility has been advanced that mechanical forces produced by pathologic hemodynamic loads may lead to myocyte cell death in the myocardium (1). This hypothesis has been made in an attempt to understand the changes in cardiac anatomy after coronary artery constriction and global myocardial ischemia, and coronary artery occlusion and myocardial infarction (1, 2). However, no documentation of this phenomenon has been obtained. This is a relevant issue because acute reductions in wall thickness and chamber dilation, as a consequence of sudden increases in ventricular end-diastolic pressure, may involve mural translocation of cells, a phenomenon commonly described as side-to-side slippage of myocytes (2). With this form of wall restructuring, the rings of cells that move radially towards the epicardial region must expand to enclose a larger cavitary volume. Since lengthening of sarcomeres and elongation of myocytes alone are inadequate to explain the increase in dimension of the ventricle (2–4), single myocyte cell death has been postulated to occur to allow side by side translocation of cells within the wall. In the absence of multiple cell death, the sliding of myocyte bundles from the inner to the outer layer of the wall would not take place, limiting mural thinning and chamber dilation. Importantly, single myocyte cell death has been claimed to be mediated by mechanical forces within the wall which may activate genes involved in apoptotic cell death (5). Therefore, experiments were conducted in an in vitro system in which abnormal resting tension levels were imposed on muscles obtained from normal adult rat hearts. The possibility was raised that the physical forces may induce apoptotic cell death in these muscles by enhancing the production of reactive oxygen species (6). Overstretching may also increase the expression of the cell surface molecule, Fas (7, 8), which has been found to be involved in apoptotic myocyte cell death (9). Since nitric oxide (NO) has been shown to decrease programmed cell death in other cell types (10) and to react with superoxide anion (11) and perhaps reduce oxidant stress (12), the beneficial effects of an NO-releasing drug (13) were examined in this setting.

Methods

Muscle mechanics. Male Sprague-Dawley rats at 3 mo of age were anesthetized with ether. Hearts were rapidly excised and placed in oxygenated Thyrode solution containing potassium to induce diastolic arrest. In each experiment, two left posterior papillary muscles were obtained from two animals and suspended side-by-side in a muscle bath. The nontendinous end of each papillary muscle was mounted to a micrometer assembly used to adjust external muscle length. The tendinous end of the papillary muscle was tied to a steel wire with Ethicon 5-0 braided silk (Ethicon, Inc., Somerville, NJ). The wire was attached to a 2-cm stainless lever connected to a servo-controlled galvanometer for measurement of isometric contraction. Muscles were perfused continuously with normal Thyrode solution maintained at 30°C by using a coiled glass heat exchanger at the inflow line in conjunction with a circulating water bath. The solution was gassed with 95% O_2/5% CO_2 (pH = 7.2). Preparations were stimulated at 0.1 Hz by rectangular depolarizing pulses 10 ms in duration and twice diastolic threshold in intensity (14).

After an equilibration period of 60–90 min, during which the muscles contracted isometrically at a resting tension of 9.8 mN/mm^2, the passive and active stress-strain relations were determined. In one group of muscles (n = 12), resting muscle length was increased step-wise until a maximal active tension was developed (L_{max}).[1] Resting length was then changed three times between L_{max} and 85% of L_{max} to assess reproductibility of the curve. In the other group of muscles (n = 14), a similar procedure was followed but initial muscle length was taken beyond L_{max}, until passive and active stress-strain relations were estab-

Address correspondence to Piero Anversa, Department of Medicine, Vosburgh Pavilion, Room 302, New York Medical College, Valhalla, NY 10595. Phone: 914-993-4168; FAX: 914-993-4406.

Received for publication 6 March 1995 and accepted in revised form 17 July 1995.

J. Clin. Invest.

0021-9738/95/11/2247/13 $2.00
Volume 96, November 1995, 2247–2259

1. *Abbreviation used in this paper:* L_{max}, maximal active tension.

lished between 106 and 85% of L_{max}. Step changes in length were made in a reproducible sequence to minimize the effects of hysteresis. Parameters dependent on muscle length were computed at intervals of 2% L_{max} by linear interpolation of the data. At the completion of each experiment, muscle length was measured with a reticle in the eyepiece of a dissecting microscope set at a magnification of 30. Muscle diameter was computed by averaging five equally spaced microscopic measurements throughout the length of the papillary muscle. The cross-sectional area was then calculated assuming the geometry of a circular cylinder. This latter parameter was also confirmed by dividing muscle weight by its length assuming a tissue density of 1.065 grams/cm^3 (14).

Histologic detection of DNA strand breaks. For this portion of the study, nine left posterior papillary muscles which had not been stretched beyond L_{max}, were positioned in the muscle bath at a fixed resting tension of nearly 7–8 mN/mm^2. A second group of 10 left papillary muscles, which had been overstretched beyond L_{max}, were maintained at a resting tension of ~ 50 mN/mm^2. These interventions were kept for a 3-h period during which muscles were stimulated as described above. At the completion of these mechanical impositions, papillary muscles were fixed for 24 h in phosphate buffered 4% formalin. Tissue was then embedded in paraffin. Sections, ~ 4 μm in thickness, were obtained from each papillary muscle and mounted on poly-L-lysine–coated slides (Sigma Chemical Co., St. Louis, MO). After deparaffinization and rehydration, tissue sections were incubated in PBS, containing 0.1% saponin and 1 mM EGTA for 30 min (5). Subsequently, sections were covered with 50 μl of staining solution containing 5 U of terminal deoxynucleotidyl transferase, 2.5 mM $CoCl_2$, 0.2 M potassium cacodylate, 25 mM Tris-HCl, 0.25% bovine serum albumin and 0.5 nM 2′-deoxyuridine-5′-triphosphate, coupled to biotin via a 16-atom spacer arm (biotin-16-dUTP). These reagents were all from Boehringer Mannheim Biochemicals (Indianapolis, IN). Sections were incubated in this solution for 30 min at 37°C in a humidified chamber. After rinsing in PBS, sections were incubated for 30 min at room temperature in a solution containing 4× concentrated SSC buffered and 5% (wt/vol) nonfat dry milk (Sigma Chemical Co.). Finally, the staining solution which contained 5 μg/ml of FITC-labeled Extravidin (Sigma Chemical Co.), 4× concentrated SSC buffer, 0.1% Triton X-100 and 5% nonfat dry milk was applied for 30 min.

Positive and negative controls were included in the protocol to confirm the specificity of the assay. As a positive control, myocardial sections were treated with DNase I to induce enzymatically the formation of DNA strand breaks. The tissue was treated with this enzyme for 15 min at 37°C and, after washing with PBS, the terminal deoxynucleotidyl transferase assay was performed. Negative controls consisted of staining for DNA strand breaks sections similarly treated in which biotin-16-dUTP or terminal deoxynucleotidyl transferase was not present. After terminal deoxynucleotidyl transferase reaction, the sections were rinsed in PBS, and stained for α-sarcomeric actin. The tissue was incubated first at 37°C for 30 min with the primary antibody (clone 5C5; Sigma Chemical Co.) diluted 1:20 in PBS, containing 10% goat serum, and subsequently with anti–mouse IgG tetramethylrhodamine B isothiocyanate (TRITC)–labeled antibody (Sigma Chemical Co.), also diluted 1:30 in PBS, containing 10% goat serum. Sections were then stained with bisbenzimide, 50 ng/ml, for 15 min to visualize nuclei. After this procedure, sections were rinsed in PBS and embedded in Vectashield (Vector Laboratories, Burlingame, CA) mounting medium.

Quantitative analysis of DNA strand breaks in myocytes and nonmyocytes. The number of myocyte nuclei in the papillary muscles labeled by biotinylated dUTP was measured by counting the number of stained nuclei per unit area of tissue sections in each papillary muscle. This analysis was performed with a microscope working in epifluorescence mode, equipped with sets of excitation emission filters for FITC (excitation blue, emission green), which allowed the identification of incorporated dUTP in nuclei. The number of labeled nuclei was recorded and the distinction between myocytes and nonmyocytes was obtained by detection of α-sarcomeric actin with the use of a second set of filters specific for TRITC (excitation green, emission red). By this approach, the number of myocytes and nonmyocytes stained by dUTP per mm^2 of tissue was determined in each muscle. Sections were examined at a magnification of 1,250 by viewing subsequent fields through the entire papillary muscle. A square tissue area equal to 6,084 μm^2 was delineated in the microscopic field by an ocular reticle (#105844; Wild Heerbrugg Instruments, Inc., Farmingdale, NY) and an average of 800 fields in each muscle were examined.

Morphometric determination of the number of dUTP-labeled myocytes and nonmyocytes. The histologic preparation described in the preceding section did not permit the determination of the fraction of myocyte nuclei labeled by dUTP. To obtain this parameter the number of myocyte nuclei and nonmyocyte nuclei per unit area of tissue was determined by counting an average of 30 fields, 6,084 μm^2 each, at a magnification of 1,250 in each papillary muscle. This analysis was performed with a microscope working in epifluorescence mode, equipped with sets of excitation emission filters for bisbenzimide H33258 (excitation UV, emission blue) and TRITC (excitation green, emission red). In randomly selected fields, nuclei were identified first (bisbenzimide staining), then excitation emission filters were changed to visualize myocytes labeled with anti–α-sarcomeric actin. In this manner, the numerical density of myocyte and nonmyocyte nuclei in each papillary muscle was obtained. By combining these data with the preceding estimations of dUTP-labeled myocyte and nonmyocyte nuclei per unit area of myocardium, the number of apoptotic myocyte and nonmyocyte nuclei per 10^6 nuclei was determined.

DNA gel electrophoresis. To confirm that the histochemical detection of DNA strand breaks corresponded to internucleosomal cleavage, the presence of low molecular weight DNA in papillary muscles was determined (15). Groups of three papillary muscles each were mechanically homogenized on ice and fixed for 24 h at −20°C in 70% ethanol. The tissue was then centrifuged at 800 *g* for 5 min and the ethanol was thoroughly removed. The pellet was resuspended in 40 μl of phosphate-citrate buffer, consisting of 192 parts of 0.2 M Na_2HPO_4 and 8 parts of 0.1 M citric acid (pH 7.8), at room temperature, for 1 h. After centrifugation at 1,000 *g* for 5 min, the supernatant was transferred to new tubes and concentrated by vacuum in a SpeedVac concentrator (Savant Instruments Inc., Farmingdale, NY) for 15 min. A 3-μl aliquot of 0.25% NP-40 (Sigma Chemical Co.) in distilled water was then added, followed by 3 μl of a solution of RNase, 1 mg/ml, also in water. After 30-min incubation at 37°C, 3 μl of a solution of proteinase K, 1 mg/ml (Boehringer Mannheim Biochemicals), was added and the extract was incubated for an additional 1 h at 37°C. After the incubation, 12 μl of loading buffer, 0.25% bromophenol blue, 30% glycerol, was added and samples were subjected to electrophoresis on 1% agarose gel containing 5 μg/ml ethidium bromide. The DNA in the gels was visualized under UV light. For this portion of the study, six nonoverstretched muscles and six overstretched muscles were utilized.

Immunohistochemical localization of Fas. Tissue sections mounted on poly-L-lysine–coated glass slides were deparaffinized by heating at 90°C followed by three washes in xylene. After dehydration in absolute ethanol for 15 s, slides were incubated in 2% (vol/vol) H_2O_2 in methanol for 30–45 s then washed with 95% ethanol for 20 s, followed sequentially by 70% ethanol for 20 s, distilled H_2O for 1 min, and PBS (120 mmol/liter NaCl, 11.5 mmol/liter NaH_2PO_4, 31.3 mmol/liter KH_2PO_4, pH 7.4–7.6) for 5 min and then heated by microwaving for 15 min. After washing twice in PBS for 5 min, tissue sections were preblocked for 45 min in TNK solution (100 mmol/liter Tris, pH 7.6–7.8, 550 mmol/liter NaCl, 10 mmol/liter KCl) containing 2% (wt/vol) BSA (Sigma Chemical Co.) 0.1% Triton X-100, and 1% normal goat serum. Antibodies were added to the slide in the same solution and incubated overnight at room temperature. Anti–mouse Fas hamster monoclonal antibody (clone Jo2; Pharmingen, San Diego, CA) was used at 1:100 (vol/vol) dilution. In some cases, the primary antibodies were omitted (negative controls). Myeloma IgG antibody (Jackson ImmunoResearch Laboratories, Inc., West Grove, PA) was also used as a second form of negative control. After washing with PBS, tissue sections were incubated for 1 h with 5 μg/ml of biotinylated goat anti–rabbit antibody (Vector Laboratories, Inc.) for the detection of Fas and then washed and incubated for 30–45 min with an avidin–biotin complex reagent containing horseradish peroxidase (Vector Laboratories, Inc.) in TNK. Color development was achieved by incubation for 10 minutes with a

solution containing 3,3′-diaminobenzidine (DAB) and 0.1% (vol/vol) H_2O_2 in TNK buffer.

The quantitative analysis of the cell localization of Fas protein was performed in 4 and 5 papillary muscles exposed to low and high levels of tension, respectively. Five equally spaced areas, along the longitudinal axis of each muscle, were samples and the number of labeled and unlabeled myocytes across the diameter of the muscle was determined in each region. These individual values were then averaged to yield a mean value in each muscle.

Detection of superoxide anion. Papillary muscle were exposed to levels of tension comparable to those described above. Under these conditions, the formation of superoxide anion was examined over a period of 3 h during which loading was kept constant. At the end of this procedure, muscles were fixed in 4% phosphate buffered formalin and embedded in paraffin for the subsequent detection of programmed cell death. Specifically, changes in force and $O_2^{\cdot -}$ generation were determined in a single photon counting apparatus constructed in a light tight box. In these experiments, stimulated muscles were incubated in Krebs' bicarbonate buffer containing 0.25 mM lucigenin in a continuously gassed 1 cm^2 spectrophotometer cuvette mounted in a thermostated cell holder on the surface of a Lucite light guide (with a shutter cover) directed into a cooled Thorn EMI Photomultiplier Tube (model 9235B; Thorn EMI Electron Tubes , Ruslip, United Kingdom). A Thorn EMI amplifier-discriminator (model C604) and photon counter (model C660) were used to quantitate chemiluminescence. The counts were integrated over 5-s periods by the photon counter, and an analog signal of the integrated counts was continuously recorded on a (model 7 Polygraph; Grass Instrument Co., Quincy, MA) recorder together with changes in force (16). This analysis was conducted in four and five muscles at low and high tension levels, respectively. The effects of superoxide dismutase on the generation of superoxide anion in overstretched muscles were also examined ($n = 4$). Moreover, the ability of *N*-2-mercaptopropionyl glycine to inhibit superoxide anion intracellulary was evaluated in four overstretched papillary muscles. For these two conditions, muscles were exposed to either superoxide dismutase, 3 μM, or *N*-2-mercaptopropionyl glycine, 2 mM, for 15 min (17, 18) before the determination of chemiluminescence levels (16). The dose of *N*-2-mercaptopropionyl glycine used here was established on the basis of preliminary experiments showing that the ability of this compound to affect superoxide anion was maximal at 2 mM without significant increases up to 20 mM.

Effects of CAS 936. The potential beneficial influence of the NO-releasing drug C87-3754, a metabolite of CAS 936 (13), on the generation of superoxide anion and the activation of programmed cell death was examined in papillary muscles. This was performed by superfusing muscles kept at low and high tension levels (see above), with a solution containing 10 μM C87-3754 during a 3-h period. The formation of reactive oxygen species was measured throughout and after the histologic preparation described above, Fas and dUTP labeling of the tissue was determined. Five muscles of high tension levels were used for chemiluminescence measurements, and seven were used for evaluation of DNA strand breaks. The effects of C87-3754 on developed and resting tensions with time were evaluated in 10 papillary muscles and compared with an identical number of muscles not exposed to the drug.

Number of myocytes across the muscle. Papillary muscles exposed to low and high levels of resting tension for a 3-h period were fixed in these conditions with a solution containing 5% glutaraldehyde and 4% paraformaldehyde. Papillary muscles were then removed and sliced transversely into four pieces which were embedded in araldite. One fragment of tissue was embedded longitudinally for the measurement of sarcomere length. Semithin sections, ~ 0.5 μm in thickness, were cut from each block perpendicular to the long axis of the muscle and showing its whole cross-sectional area. The transverse area was determined by an interacting tracking device and the mean diameter was computed (Jandel Scientific, Corte Madera, CA). Subsequently, thin sections were obtained from these blocks and low power electron micrographs, four from each of two blocks from each papillary muscle, were collected. These micrographs were printed at a final magnification of 4,500 and the volume composition of the myocardium and the numerical density of myocyte profiles per unit area of tissue were measured as previously described (2). The availability of papillary muscle diameter and myocyte density allowed the calculation of the number of cells across the papillary muscle (2). The mean center-to-center distance (d_{c-c}) between myocytes was calculated from the number of profiles counted per unit area of tissue, ($N_{(m)A}$) in transverse myocardial sections by assuming the tendency for these roughly cylindrical cells to pack in a close hexagonal pattern (2):

$$d_{c-c} = \sqrt{\frac{2}{\sqrt{3} \cdot N_{(m)A}}} = \frac{1.0746}{\sqrt{N_{(m)A}}}$$

In a hexagonal pattern, the spacing between planes of adjacent cells varies with the orientation of the array from a maximum of d_{c-c} to a minimum of $d_{c-c}\sqrt{3}/2$ and has a mean value, d, representative of random orientation, given by

$$d_{c-c} = \frac{3d_{c-c}\sqrt{3}}{\pi} \int_0^{\pi/6} \frac{d\theta}{\cos\theta} = 0.9085\ d_{c-c}$$

Thus, the number, $N_{(m)tm}$, of myocytes across the thickness of the papillary muscle, W, can be found from

$$N_{(m)tm} = W/d = 1.0243 \cdot W \cdot \sqrt{N_{(m)A}}$$

This analysis was performed in six muscles at low and six muscles at high tension levels. The block of tissue embedded parallel to the major axis of the papillary muscle was sectioned and sarcomere length in myofibrils was determined in each muscle from 100 measurements made at a magnification of 30,000. These sections were longitudinally oriented and were cut perpendicular to their length to avoid longitudinal compression.

Data collection and analysis. All tissue samples were coded, and the code was broken at the end of the experiment. Results are presented as mean±SD computed from the average measurements obtained from each muscle. Comparisons between two values were performed using a two-tailed Student's *t* test. Statistical significance in multiple comparisons in which the analysis of variance and the *F* test indicated the presence of significant differences was determined by the Bonferonni method. Values of $P < 0.05$ were considered significant.

Results

Muscle mechanics. Fig. 1 illustrates the passive and active length tension relationships of papillary muscles between 85 and 100% of L_{max}, and between 85 and 106% of L_{max}. Muscles stretched up to 100% of L_{max} showed that the progressive increase in resting tension was coupled with a parallel increase in developed tension which peaked at L_{max} (Fig. 1 *A*). These muscles maintained their ability to generate expected levels of developed tension upward and downward along the entire length tension curve. In contrast, papillary muscles stretched beyond L_{max} exhibited marked increases in resting tension associated with a decrease in isometric developed tension (Fig. 1 *B*). From 100 to 106% of L_{max}, resting tension increased from a value of 19 mN/mm^2 to a value of 52 mN/mm^2. In contrast, isometric developed tension decreased from a value of 73 mN/mm^2 to a value of 61 mN/mm^2. These differences were both statistically significant ($P < 0.001$). Moreover, overstretched papillary muscles were unable to produce the same developed tensions and when moved downward along the length, tension relationships produced less tensions throughout the range of physiologic loads examined. The resting tension curve was shifted to the right at all lengths from 104 to 94% of L_{max} ($P < 0.001$), whereas the reductions in developed tension were statistically significant from 102 to 85% of L_{max} ($P < 0.001$).

Fig. 2 depicts the time-dependent changes in resting and

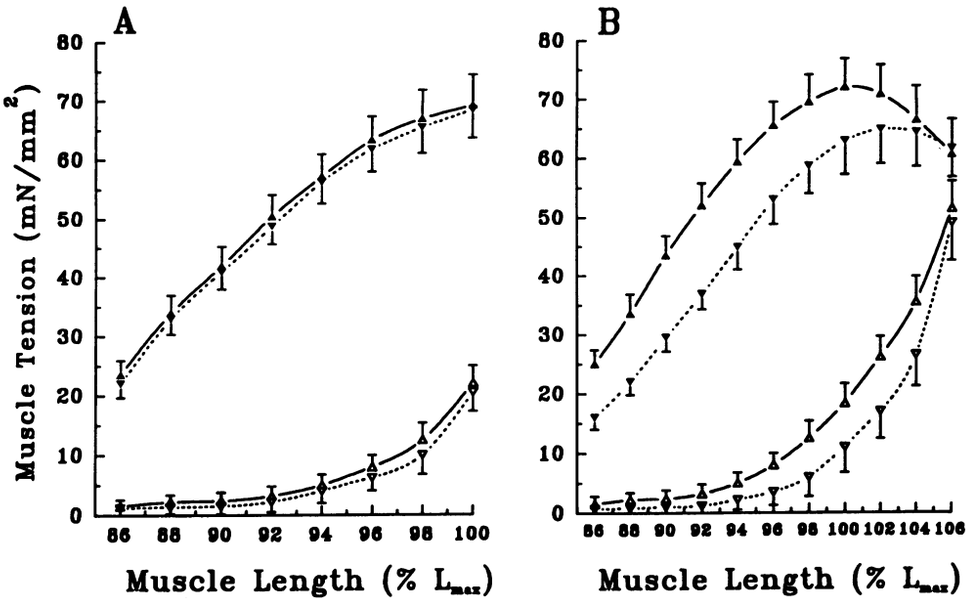

Figure 1. Resting and active length tension relationships of left posterior papillary muscles. Muscles extended beyond L_{max} (n = 14) were not able to maintain stable levels of resting and developed tensions (B). This phenomenon was not present in muscles extended up to L_{max} (n = 12) (A). Results are presented as mean±SD. (▲) Corresponds to active tension development at increasing muscle lengths; (▼) corresponds to active tension development at decreasing muscle lengths; (△) corresponds to resting tension development at increasing muscle lengths; and (▽) corresponds to resting tension development at decreasing muscle lengths. See text for statistics and more details.

developed tensions in papillary muscles exposed to resting tension levels of ~ 7–8 and 50 mN/mm^2, respectively. Moderately stretched papillary muscles maintained comparable levels of passive and active tensions over a 3-h period. Conversely, overstretched muscles showed an initial increase in isometric developed tension followed by a progressive decline with time. Resting tension in these muscles decreased continuously during the 3-h interval. In summary, overstretching affected the ability of papillary muscles to maintain stable levels of resting and developed isometric tensions with time.

Structural characteristics. Semithin sections of papillary muscles showed that the normal structure of muscles was preserved in all cases. Thus, consistent with previous results (19), the size of the muscles used in this study did not limit oxygenation of the core of the muscles producing cellular damage. This was confirmed quantitatively, since the volume fraction of myocytes and interstitial compartment in muscles exposed to moderate levels of tension was 86±1.0 and 14±1.0, whereas the corresponding values in muscles kept at high tension were 87±2.0 and 13±2.0. Measurements of papillary muscle cross-sectional area were obtained from these histologic preparations for the subsequent evaluation of papillary muscle diameter. High resting tension levels were associated with an 8% reduction in muscle diameter which, however, was not statistically significant (Fig. 3 *A*).

The numerical density of myocyte profiles per unit area of papillary muscle was obtained by low power electron microscopy. Myocyte numerical density was 5,405±344 in muscles maintained for 3 h at 7–8 mN/mm^2 and 4,857±444 in muscles kept for the same time at 50 mN/mm^2. These values, in combination with the volume fraction of myocytes in the tissue, were utilized to compute the average cross-sectional area and diameter of myocytes. In comparison with muscles subjected to moderate loads, high loads were characterized by a 13 and 6%

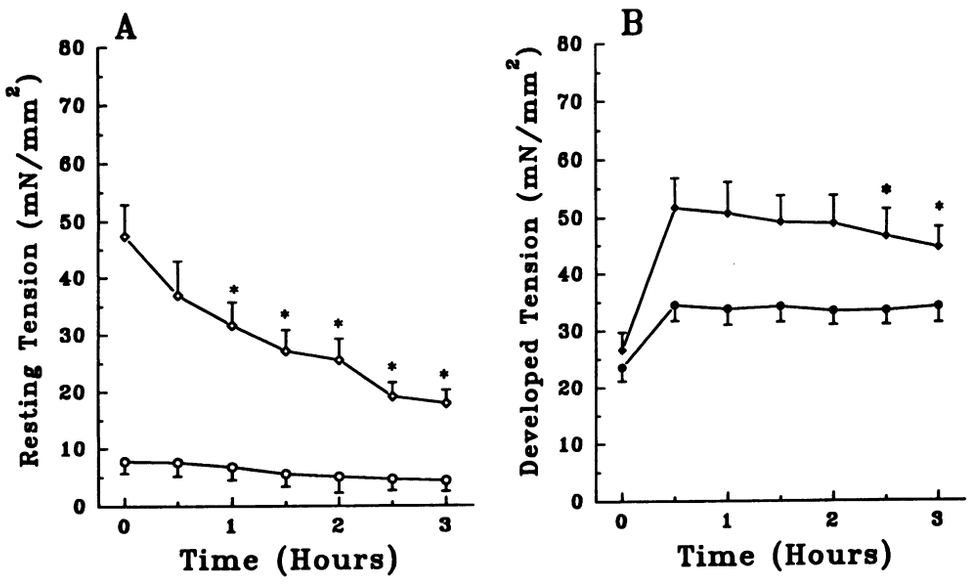

Figure 2. Effects of loading, ~ 7–8 mN/mm^2 (n = 9) and 50 mN/mm^2 (n = 10) on resting and developed tension with time. * Indicates a value that is statistically significantly different from the value obtained at 30 min, $P < 0.05$.

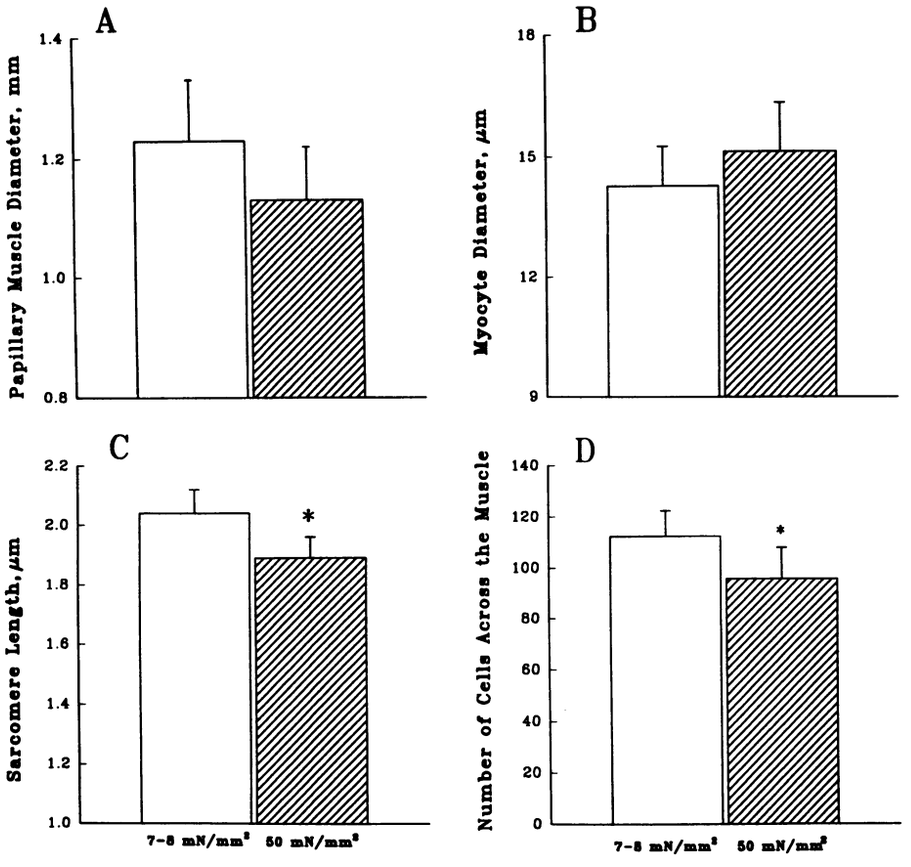

Figure 3. Effects of loading, ~ 7–8 mN/mm^2 (n = 6) and 50 mN/mm^2 (n = 6) for a 3-h period, on papillary muscle diameter (A), myocyte diameter (B), sarcomere length (C), and number of myocyte profiles within the thickness of the papillary muscle (D). Results are presented as mean±SD. * Indicates a value that is statistically significantly different, $P < 0.05$.

greater myocyte transverse area and diameter, respectively. However, these changes were not statistically significant (Fig. 3 B). On the other hand, sarcomere length measured in longitudinally oriented sections of myocytes was 7% shorter in overloaded muscle (Fig. 3 C) and this difference was statistically significant ($P < 0.01$). When the number of myocytes across the diameter of the papillary muscle was computed according to the equation in the Methods section, muscles maintained at 50 mN/mm^2 were found to possess 15% less myocyte profiles than muscles kept at 7–8 mN/mm^2 (Fig. 3 D). This difference was statistically significant ($P < 0.02$). In summary, high tension levels reduced the number of myocyte profiles within the thickness of the papillary muscle.

Biotinylated dUTP detection in the papillary muscle. The specificity of the technique utilized to stain DNA strand breaks in different cell populations was documented by treating tissue sections with DNase I before the detection of DNA strand breaks by dUTP labeling (Fig. 4, A and B). Conversely, DNA strand breaks were not detected when biotin-16-dUTP (Fig. 4, C and D) or terminal deoxynucleotidyl transferase was not included in the enzymatic reaction. An identical effect was also obtained by staining sections which contained DNA strand breaks in the absence of biotin-16-dUTP or terminal deoxynucleotidyl transferase.

Fig. 5 illustrates the localization of DNA strand breaks in myocyte nuclei of left posterior papillary muscles maintained for 3 h at 50 mN/mm^2. Occasional dUTP-stained myocyte nuclei were also seen in muscles kept at 7–8 mN/mm^2. However, the number of positively labeled myocyte nuclei was greater in muscles exposed to higher tension levels. Interstitial cells were also found to be labeled by dUTP and the number of apoptotic nonmyocyte nuclei also increased in overstretched muscle preparations. In contrast, after treatment with C87-3754, dUTP labeling of myocytes and nonmyocytes in muscles maintained at 50 mN/mm^2 was significantly reduced, reaching values similar to those of muscles kept at 7–8 mN/mm^2. To avoid potential influences from the damaged ends of the muscle, this analysis was restricted to the mid-portion of each papillary muscle.

Fig. 6 shows quantitatively the effects of overstretching and C87-3754 on the number of myocyte nuclei and nonmyocyte nuclei exhibiting DNA strand breaks in papillary muscles. After a 3-h period of exposure of muscles to high tension levels, 6,400 myocyte nuclei per 10^6 nuclei exhibited DNA strand breaks. This value was 21-fold higher than that obtained in muscles kept at moderate tension, 300 myocyte nuclei per 10^6 nuclei. This difference was statistically significant ($P < 0.001$). In addition, overstretching was associated with a 2.4-fold increase in the number of interstitial cells labeled by dUTP. This difference was also statistically significant ($P < 0.02$). Conversely, C87-3754 was capable of maintaining the extent of dUTP labeling of myocytes and nonmyocytes within values comparable to those found at moderate tension, in spite of the overstretching. In summary, overstretching was associated with a 21-fold and a 2.4-fold increase in the magnitude of dUTP labeling of myocytes and nonmyocytes in papillary muscles and C87-3754 prevented this phenomenon.

Detection of DNA laddering in the myocardium. The presence of DNA fragments of size equivalent to the mono or oligonucleosomes was determined to confirm the detection of DNA strand breaks in myocyte nuclei. Because only a relative small fraction of myocytes was undergoing apoptosis in the overstretched papillary muscles, a procedure for extraction of low

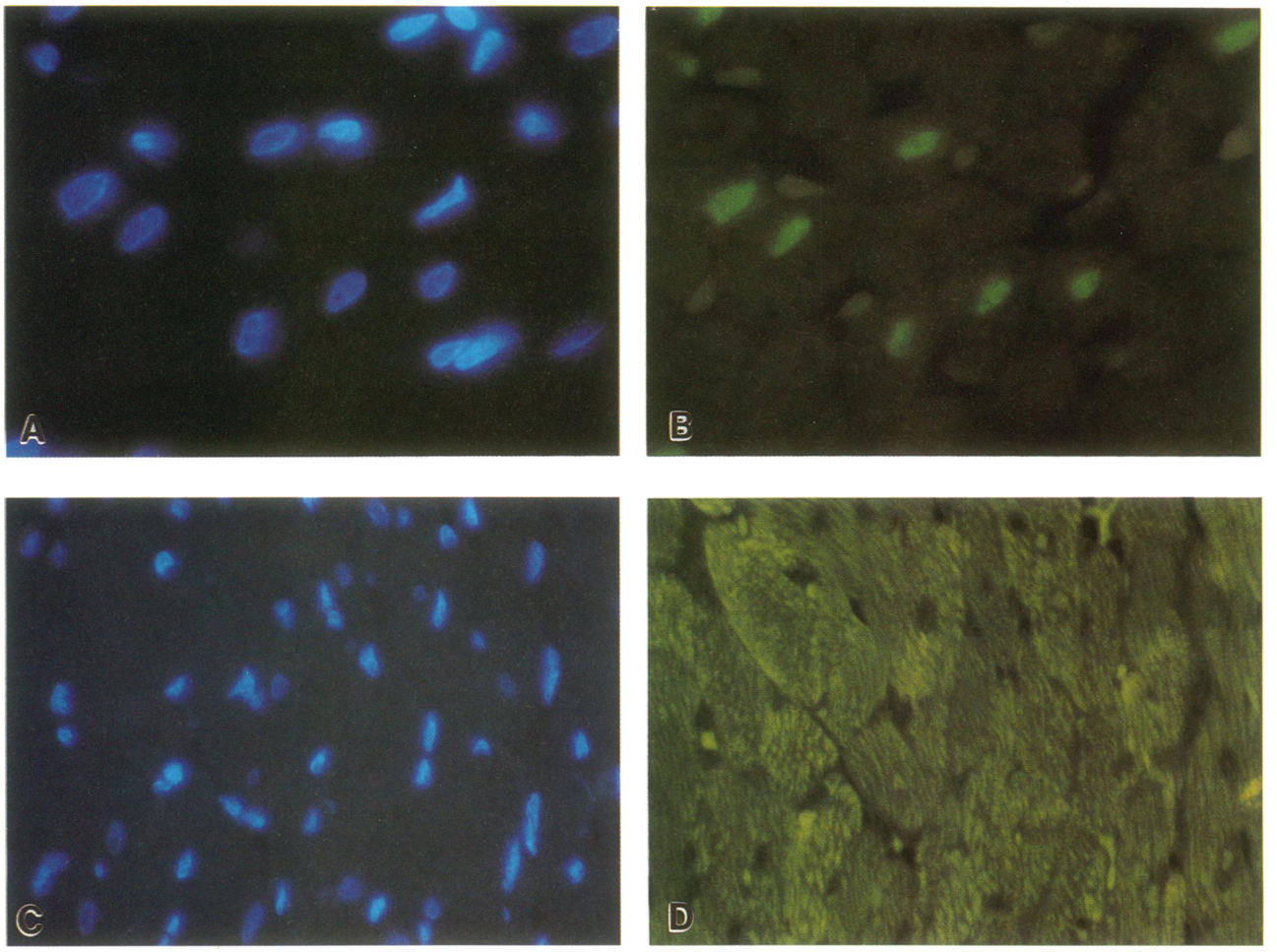

Figure 4. Detection of DNA strand breaks in nuclei after treatment of sections of myocardium with DNase I. (*A*) Illustrates by bisbenzimide fluorescence, the nuclei included in the section, whereas (*B*) shows that most nuclei were stained by biotinylated dUTP after DNase exposure. Omission of dUTP from the reaction results in negative staining (compare *C* with *D*). The contrast in (*D*) was enhanced to demonstrate more clearly the lack of dUTP labeling. (*A–D*) ×400.

molecular weight DNA from apoptotic cells was used (15). As illustrated in Fig. 7, extracts obtained from the muscles exposed to 50 mN/mm^2 revealed the presence of DNA fragments consistent with apoptosis. Stretches of DNA of size equivalent to 200 bp were the most abundant. Moreover, 400-, 600-, and 800-bp fragments which correspond to two, three, and four nucleosomes, respectively, were also visible. In contrast, no degradation of DNA was found in nonoverstretched papillary muscles. In summary, DNA fragmentation characteristic of apoptotic cell death was observed in overstretched papillary muscles.

Chemiluminescent measurement of superoxide anion generation. To determine whether overstretching of the papillary muscle was associated with an enhanced formation of reactive oxygen species, lucigenin-dependent photoemission was measured in muscles kept for 3 h at 7–8 and 50 mN/mm^2. As illustrated in Fig. 8, papillary muscles exposed to the lower level of tension exhibited no changes in the formation of superoxide anion during the 3-h period of stretching. In contrast, overstretching resulted in a marked elevation of superoxide-elicited lucigenin chemiluminescence. When these two values were compared, a 2.7-fold higher activation of superoxide formation was found in muscles at 50 mN/mm^2 ($P < 0.005$) than in muscles at 7–8 mN/mm^2. To establish whether NO was able to prevent stretch-induced superoxide generation, a separate group of overstretched papillary muscles was exposed to 10 μM C87-3754. As shown in Fig. 8, in the presence of the NO-releasing drug, a 42% ($P < 0.02$) decrease in the formation of superoxide anion was noted. To confirm the intracellular origin of superoxide anion, the effects of superoxide dismutase and *N*-2-mercaptopropionyl glycine on overstretched muscles were measured. Superoxide dismutase did not affect the level of chemiluminescence generated by the overstretched muscles. This intervention decreased the formation of superoxide anion by 2.65±4.51% ($n = 4$) which was not statistically significant. In contrast, *N*-2-mercaptopropionyl glycine reduced this parameter by 53.51±11.64% ($n = 4$) and this change was statistically significant ($P < 0.01$).

Fig. 9 illustrates the values of active and resting tensions of papillary muscles exposed to a load of ~ 50 mN/mm^2, in the presence and absence of C87-3754. This phenomenon was examined over a 3-h period. The NO-releasing drug was associated with lower levels of developed tension than those observed in the absence of C87-3754, in spite of a comparable magnitude of preload. Resting tension was similar in both groups of muscles. Moreover, developed and resting tension decreased with time in the absence of the drug intervention, whereas no statisti-

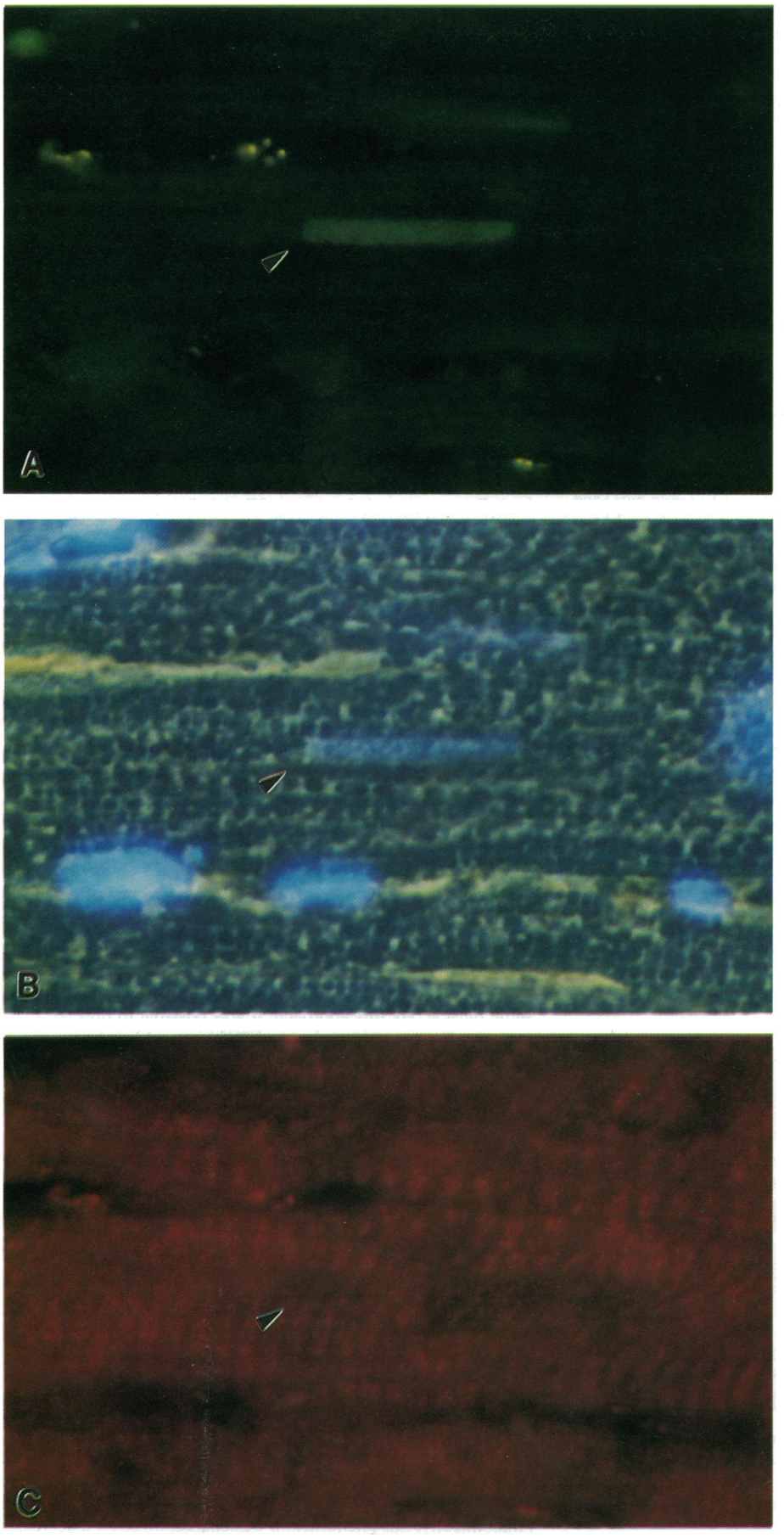

Figure 5. Detection of DNA strand breaks in a myocyte (*A*) nucleus (*arrowhead*) by biotinylated dUTP labeling of an overstretched papillary muscle. (*B*) Illustrates the same microscopic field by a combination of phase contrast and bisbenzimide fluorescence. Myocytes were identified by labeling with α-sarcomeric actin antibody (*C*). (*A–C*) ×1,200.

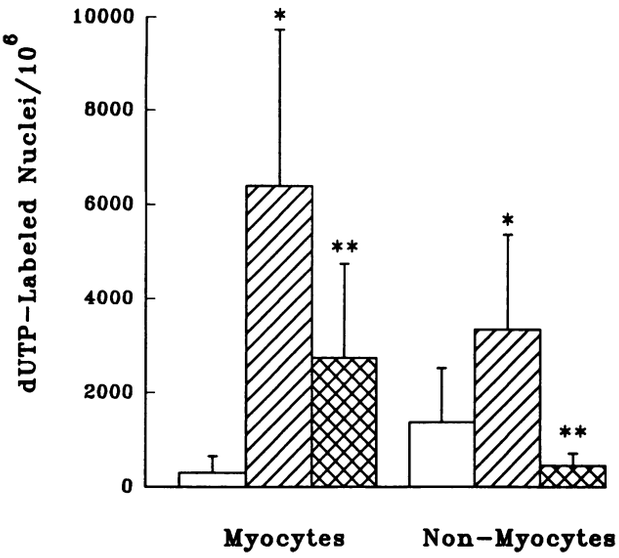

Figure 6. Effects of loading, ~ 7–8 mN/mm^2 (n = 9) (*open bars*) and 50 mN/mm^2 (n = 10) (*hatched and cross-hatched bars*) for a 3-hr period, in the presence (n = 7) (*cross-hatched bars*) and absence (*open and hatched bars*) of CAS 936 on the number of dUTP-labeled nuclei per 10^6 cells in papillary muscles. Results are presented as mean±SD. * Indicates a value that is statistically significantly different from the value in muscles exposed to nearly 7–8 mN/mm^2, $P < 0.05$. ** Indicates a value that is statistically significantly different from the value in muscles exposed to ~ 50 mN/mm^2, $P < 0.05$.

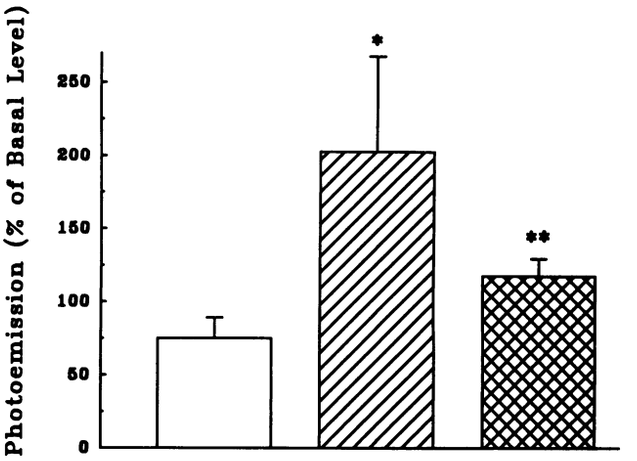

Figure 8. The relative change in superoxide anion–elicited lucigenin chemiluminescence after 3-h exposure of papillary muscles to 7–8 mN/mm^2 (n = 4) (*open bar*), 50 mN/mm^2 (n = 5) (*hatched bar*), and 50 mN/mm^2 in the presence of 10 μM CAS 936 (n = 7) (*cross-hatched bar*). Data are presented as mean±SD * Indicates a value that is significantly different from muscles exposed to 7–8 mN/mm^2 ($P < 0.05$). ** Indicates a value that is significantly different from muscles exposed to 50 mN/mm^2, $P < 0.05$.

cally significant changes in these parameters occurred during the 3-h interval examined with C87-3754. In summary, overstretching was characterized by enhanced formation of superoxide anion intracellularly and this effect was attenuated by an NO donor which also maintained active and passive tension levels stable over time.

Expression of Fas in papillary muscles. Fig. 10, *A–C* illustrate the localization of Fas protein in myocytes of muscles exposed to 7–8 and 50 mN/mm^2, respectively. Although immunostaining for Fas was only occasionally observed in myocytes of muscles maintained at 7–8 mN/mm^2 (Fig. 10 *A*), numerous myocytes were labeled in muscles kept at 50 mN/mm^2 (Fig. 10, *B* and *C*). In contrast, Fas labeling was not detected in interstitial cells of the same muscles. The specificity of immunostaining for Fas was confirmed by the lack of labeling when sections were processed in the absence of the primary antibody (Fig. 10 *D*) or in the presence of myeloma IgG antibody (Fig. 10 *E*). It should be emphasized that tissue sections could not be stained simultaneously for DNA strand breaks and Fas protein because dUTP labeling required 0.2 M cacodylate buffer which interferes with Fas immunolabeling. Conversely, retrieval of Fas antigen requires microwaving which induces DNA strand breaks (not illustrated). However, attempts were made to document Fas labeling and dUTP staining in serial sections of the same muscle. By this approach, it was possible to observe that, at times, Fas overexpression and DNA strand breaks involved the same muscle cell profiles (Fig. 10, *F–I*). Quantitatively, the number of myocytes labeled by Fas was 67,000±26,000 per 10^6 cells in overstretched muscles and 3,200±2,400 per 10^6 cells in nonoverstretched muscles. This difference was statistically significant ($P < 0.003$). Importantly, C87-3754 treatment reduced the number of Fas-labeled myocytes in overstretched muscle to 7,800±2,300 per 10^6 cells. The 88% decrease in Fas labeling of myocytes was statistically significant ($P < 0.01$). The addition of C87-3754 resulted in a level of Fas labeling in overstretched muscles similar to that measured in nonoverstretched muscles ($P = 0.1$). In summary, overstretching was associated with an increase in the expression of Fas in myocytes which was markedly attenuated by an NO donor.

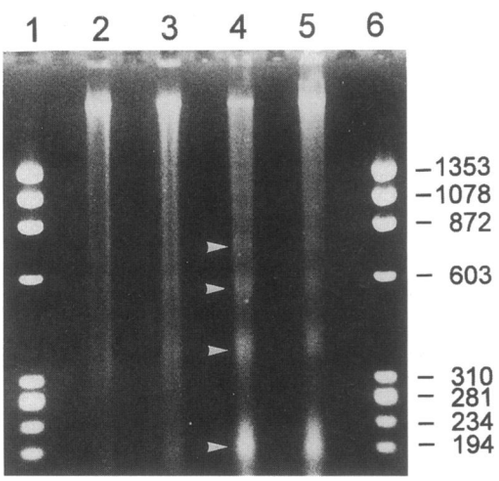

Figure 7. Electrophoretic pattern of DNA fragments extracted from nonoverstretched (lanes *2* and *3*) and overstretched (lanes *4* and *5*) papillary muscles. Lanes *1* and *6*, molecular weight markers. Each lane corresponds to three papillary muscles. Arrows correspond to 200-, 400-, 600-, and 800-bp DNA fragments.

Discussion

The results of the current study indicate that the force generating ability of papillary muscles exposed to high levels of resting tension decreased along the entire length tension relationship. Anatomically, this phenomenon was characterized by a decrease

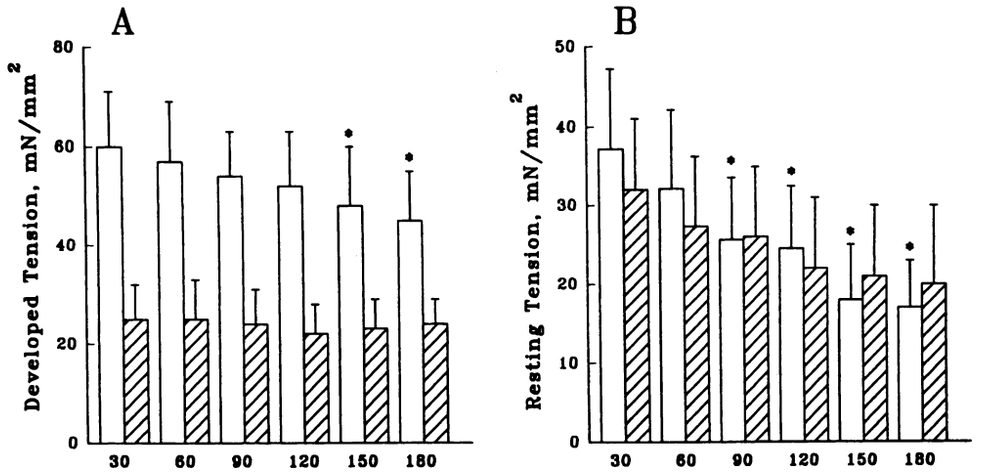

Figure 9. Effects of loading, ~ 50 mN/mm^2, in the absence (n = 10) (*open bars*) and presence (n = 10) (*hatched bars*) of CAS 936 on active (*A*) and passive (*B*) tension with time. Results are presented as mean±SD. * Indicates a value that is statistically significantly different from the value obtained at 30 min, $P < 0.05$.

in muscle diameter, apoptotic myocyte and nonmyocyte cell death, and a reduction in the number of muscle cells within the thickness of the papillary muscle. Moreover, endogenous superoxide production was increased. At the molecular level, an enhanced expression of Fas receptor protein was documented in myocytes. Thus, the possibility may be raised that pathologic alterations of myocardial load may be coupled with the generation of reactive oxygen species and the activation of gene products implicated in programmed cell death. In turn, this phenomenon may lead to an architectural rearrangement of the myocardium involving side-to-side slippage of myocytes. Importantly, interventions resulting in the release of NO prevented the formation of superoxide anion, Fas protein, programmed cell death and the relative reduction in muscle performance associated with the imposition of abnormal mechanical loads.

Mechanical performance of the myocardium. Along the ascending limb of the cardiac length-tension curve, developed tension is length dependent and this property is related to the calcium activation of myofilaments mediated by the troponin–tropomyosin protein regulatory complex (20, 21). The overlapping of thin and thick filaments is unchanged in the positive portion of the Frank–Starling relation (22), and the changes in resting length and force development are related to the extent of calcium myofilament interaction (22, 23). However, less understood are the mechanisms implicated in the alterations in resting and active tensions observed in muscles exposed to levels of stretch beyond the peak of the length-tension curve (22). Under this setting, excessive passive forces are generated and damage has been claimed to occur to the ends of the muscle preparations affecting tension development (22). Misalignment of sarcomeres and/or slippage of myofibrils within the cells have been considered to represent the in vivo counterpart of these in vitro conditions mimicking pathologic states of the heart (24).

Observations in the current study document that high loads altered the contractile behavior of the myocardium and this phenomenon was characterized by a reduction in muscle diameter. Importantly, sarcomere length was longer in muscles fixed at moderate than high loads. Damage to the myocyte and nonmyocyte compartments of the muscle was not observed in either case. In addition, the lack of register between individual myofibrils in the cytoplasm was a consistent finding in both preparations, raising questions on the role played by this structural modification in the depression of force generation in overstretched papillary muscles. The decrease of sarcomere length in muscles kept for a 3-h period at 50 mN/mm^2 suggests that the mechanical imposition shifted the muscle downward on the length tension relationship resulting in a decrease in tension development. This notion is consistent with a slight reduction in sarcomere length at higher loads.

Ventricular dilation after increases in filling pressure in the intact heart in vitro, acute and chronic ventricular dysfunction, acute and chronic myocardial infarction, sudden restrictions in coronary perfusion with global myocardial ischemia, and during the alterations in loading associated with the transition from the fetal to the adult circulatory system (for review see reference 25) has all been considered to be characterized by a structural reorganization of the myocyte compartment of the myocardium, resulting in mural thinning and expansion in cavitary volume. This adaptation, consisting of side-to-side slippage of cells within the wall, appears to be the principal determinant of acute ventricular dilation under these pathologic conditions of the heart. In a few cases, a decrease in the number of myocytes included in the thickness of the ventricular wall has been demonstrated quantitatively (2, 26) in an attempt to support the notion of mural translocation of cells. Findings in the current study demonstrate that abnormal mechanical forces resulted in a reduction in the number of cells within the width of the papillary muscle, providing the first documentation that load and myocyte slippage are causally related.

Programmed myocyte cell death. Although very little is known concerning programmed cell death in the myocardium (5, 27), this phenomenon affects various cell types and is initiated by a variety of environmental stimuli (28). During this process, an important factor is the activation of an endogenous endonuclease which results in endonucleolysis (28). DNA degradation, triggered by this mechanism, is specific to the spacer regions, leaving the DNA associated with the nucleosomes intact (29). The technique used here allowed an early detection of DNA strand breaks in myocardial cell nuclei by the terminal deoxynucleotydil transferase assay (28). Moreover, the morphologic documentation of apoptotic cell death was confirmed by the demonstration of intranucleosomal cleavage by the DNA laddering assay. Similar observations have been made after ischemic reperfusion injury of the rabbit heart in vivo (27), and in neonatal cardiac myocytes in culture exposed to hypoxic condition (9). However, defects in oxygen diffusion to the papillary muscle in our preparation were unlikely, suggesting that pro-

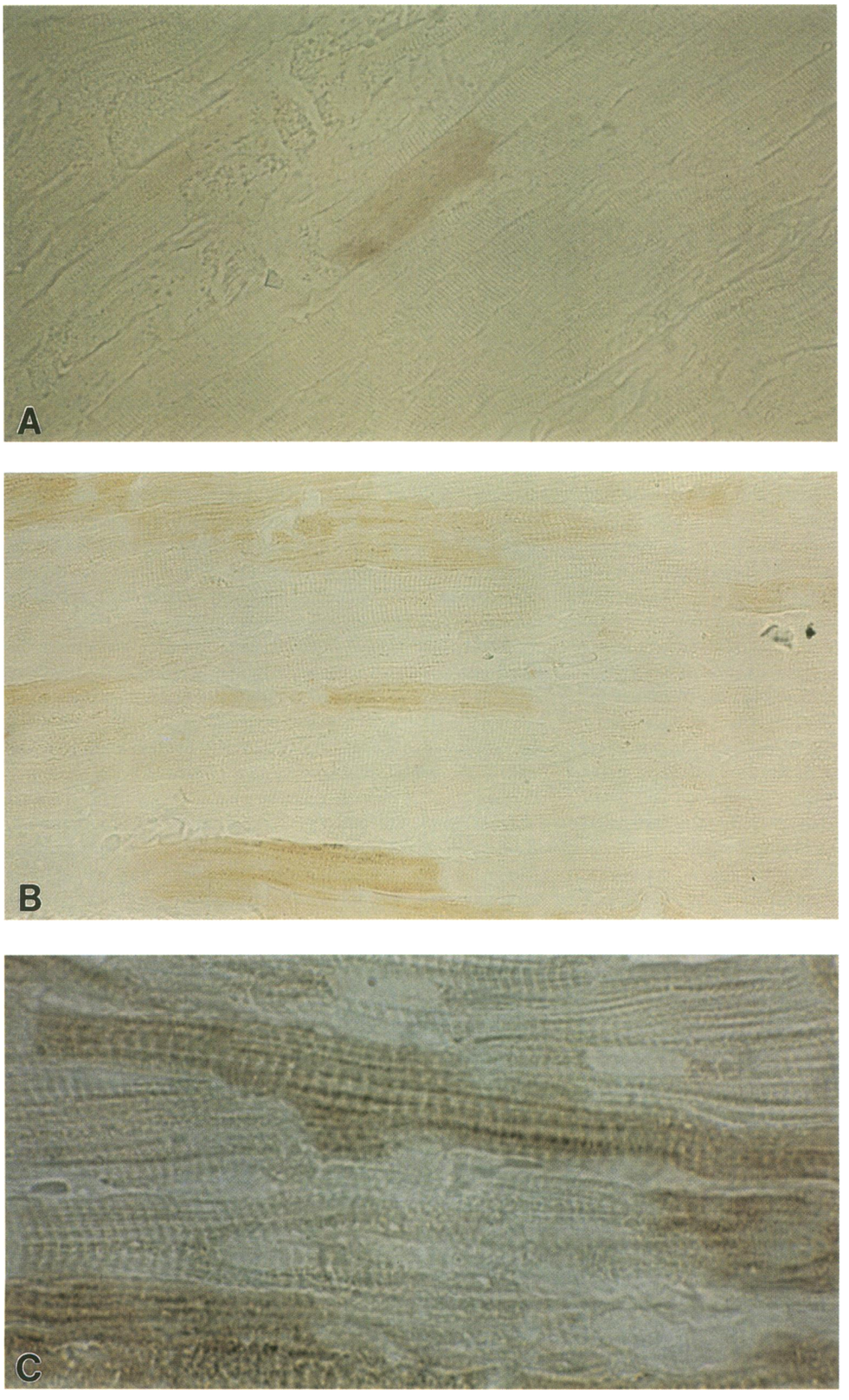

Figure 10. Photomicrographs illustrating Fas monoclonal antibody labeling of a nonoverstretched (*A*) and an overstretched (*B* and *C*) papillary muscle. Omission of the primary antibody (*D*) or its substitution with myeloma IgG antibody (*E*) during the reaction resulted in negative staining of an overstretched muscle. Serial sections of an overstretched papillary muscle showing dUTP labeling (*F* and *H*) and Fas labeling (*G* and *I*) of the same cells (*arrows*). (*A* and *B*) ×400; (*C*) ×1,100; (*D–I*) ×600.

grammed cell death occurred via a different mechanism. Ischemic myocyte cell death is characterized by rupture of the sarcolemmal lining, contraction bands in myofibrils, and mitochondrial swelling (28–30). Loss of membrane function (28) and mitochondrial swelling are distinct aspects of necrotic cell death in all cell populations (28, 30). In contrast, programmed cell death typically occurs in the absence of loss of plasma membrane integrity and function (28–30). The morphology of mitochondria in apoptotic cells is also unchanged. Findings in this study, documenting the lack of alterations at the level of the

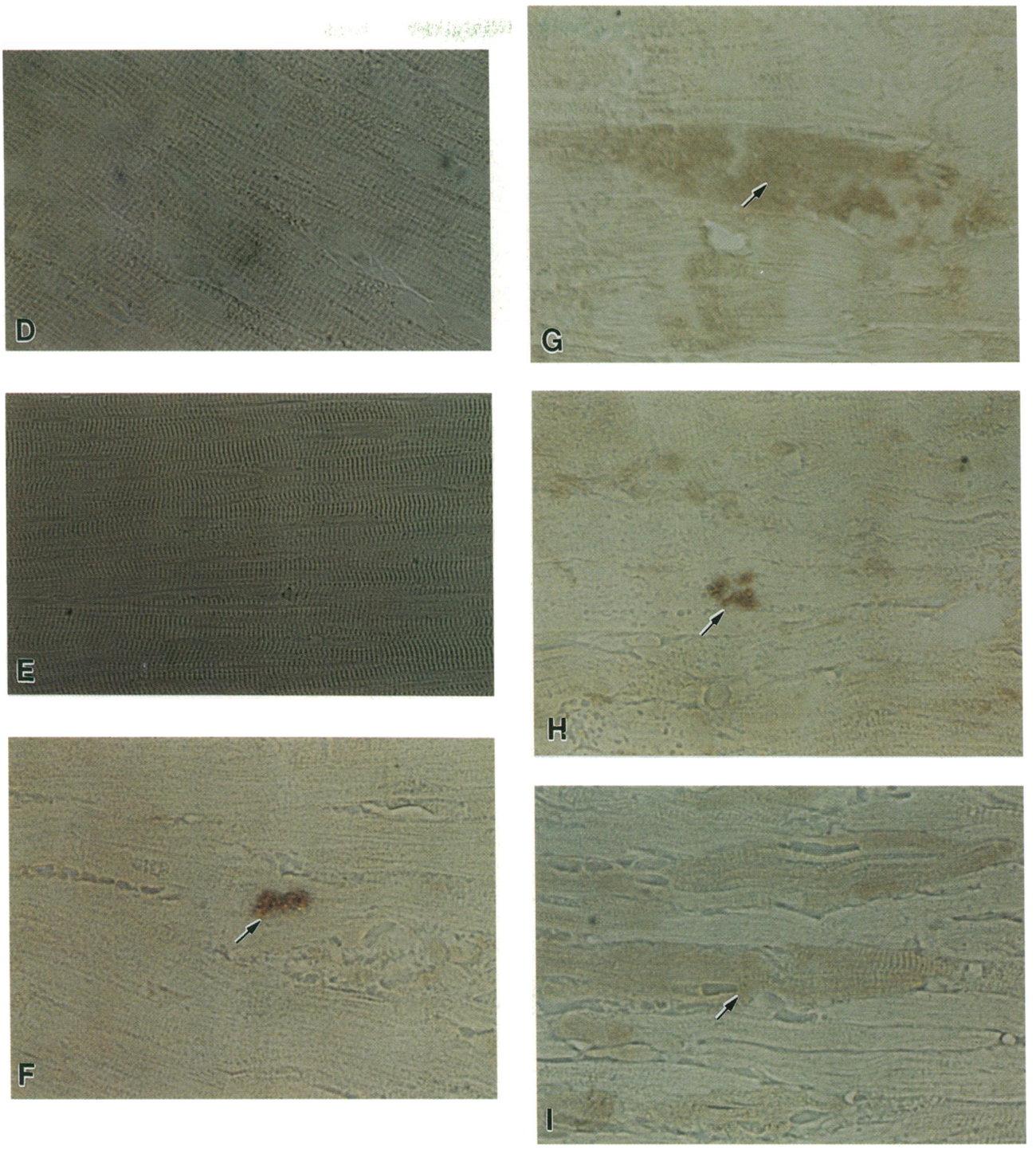

Figure 10 (Continued)

plasma membrane, myofibrils and mitochondria, indicate that the protocols used did not produce necrotic cell death in the papillary muscles. In addition, apoptotic cell death appeared to be independent from local ischemia. DNA strand breaks in myocyte and nonmyocyte nuclei were detected in the absence of structural abnormalities at the light and electron microscopic levels, suggesting that 3 h of mechanical stretching produced lesions characteristic of the early phases of apoptotic cell death.

The observation that overstretching triggered programmed cell death, involving nearly 0.5% of myocytes, raises the possibility that loss of contractile function in these apoptotic cells may have influenced the detrimental impact of high loading states on isometric tension development of the myocardium. Although the percentage of cells affected by this phenomenon was less than the reduction in active tension, single cell death may have impinged upon the force generating ability of neighboring cells depressing more severely overall muscle performance. DNA laddering clearly showed the presence of 200-, 400-, 600-, and 800-bp fragments of DNA in the overstretched muscles, but the actual magnitude of programmed cell death in

the tissue cannot be calculated from these observations. Similarly, dUTP labeling of myocytes provides an estimation of the early events of apoptosis only (28). Thus, the percentage of myocytes labeled by dUTP most likely represents an underestimation of the real extent of myocyte cell death in the tissue (5). As indicated above, myocyte slippage was accompanied by a decrease in sarcomere length, modifying the passive and active length tension relationships. However, the relative contribution of programmed myocyte cell death and myocyte slippage to the impairment in myocardial performance in overstretched papillary muscles cannot be determined at present. On the other hand, these events characterize a common pathophysiologic phenomenon in which abnormal loads trigger programmed myocyte cell death which leads to side-to-side slippage of myocytes depressing muscle contractile behavior.

The magnitude of apoptotic myocyte death in overstretched muscle was lower than the extent of myocytes expressing Fas protein on the surface of the cell and cytoplasm. Fas protein was barely detectable in myocytes of moderately loaded muscles, indicating that its expression was dependent upon the extent of load imposed on the myocardium. Although a cause and effect relationship between programmed myocyte cell death and the Fas molecule cannot be claimed, it is noteworthy that Fas mRNA increases in neonatal cardiac myocytes in culture undergoing programmed cell death (9). The *Fas* gene belongs to the tumor necrosis factor and nerve growth factor receptor family (7–9) and apoptosis can be triggered by ligand activation of the Fas receptor (8). Whether stressed myocytes can generate the Fas ligand triggering their own suicide program is currently unknown. Although the lack of Fas labeling in fibroblasts of overstretched muscles was unexpected, this phenomenon appears to be consistent with the moderate increase in apoptotic cell death of the interstitial cell population of the myocardium under this setting.

Reactive oxygen species, NO, and programmed cell death. Impositions of high loads on the myocardium are characterized by an increased oxygen consumption and this phenomenon may lead to the generation of superoxide anion which may activate the suicide program of myocytes and interstitial cells (6). NO may counteract superoxide exerting a protective influence against apoptotic cell death in vitro (10). The results of the current study are consistent with this contention, since the NO-releasing drug, C87-3754, was capable of preventing the formation of DNA strand breaks in myocytes and interstitial cells of papillary muscles exposed to high levels of tension. In addition, the preservation of myocardial structural integrity was associated with the maintenance of resting and active tension values of overstretched muscles with time. Thus, NO salvaged the myocardium from the detrimental impact of overstretching, functionally and morphologically.

Although it is difficult to recognize, at present, the effector pathway that couples abnormal mechanical loads, enhanced expression of Fas, programmed cell death and muscle restructuring, the observations with NO release point to the induction of superoxide as a relevant factor in the initiation of this cascade of events. Several cellular mechanisms can form reactive oxygen species, including the conversion of xanthine dehydrogenase to xanthine oxidase in reperfusion injury (31), mixed-function oxidase systems (32), and electron transport in the respiratory chain (33). Whether one or multiple cellular processes contributed to myocardial injury in the overstretched papillary muscle remains to be determined. NO may alleviate oxidant stress and thereby protect from apoptosis (34, 35). However, NO administration markedly reduced the extent of tension development in the overloaded papillary muscle, and this negative inotropic effect may have contributed to diminish the damaging impact of a load of 50 mN/mm^2 on the structure and function of myocytes. This reduction in muscle performance is consistent with observation in vivo (36–38) and in vitro (39, 40), indicating that NO reduces oxygen consumption and decreases myocardial contractility.

In conclusion, abnormal levels of resting tension appeared to be associated with the activation of the suicide program of myocytes and reduction in muscle mechanical performance. In addition, an architectural rearrangement of the myocyte compartment occurred, and this phenomenon of restructuring, in combination with apoptotic cell death, may have contributed to depress the mechanical behavior of the myocardium. The intracellular formation of superoxide anion and the overexpression of Fas protein in myocytes may have been the critical factors in the initiation of the cascade of events leading to programmed cell death and alteration in myocardial contractility. NO seemed to protect from these detrimental effects of overstretching.

Acknowledgments

The expert technical assistance of Maria Feliciano and the assistance of Dr. Pawel Kaminski in adapting the superoxide quantitation methods are greatly appreciated.

This work was supported by grants HL-38132, HL-39902, HL-40561, HL-50142, HL-53053, HL-31069, and PO-1-HL-43023 from the National Heart, Lung and Blood Institute.

References

1. Capasso, J. M., M. J. Jeanty, T. Palackal, G. Olivetti, and P. Anversa. 1989. Ventricular remodeling induced by acute nonocclusive constriction of coronary artery in rats. *Am. J. Physiol.* 257:H1983–H1993.

2. Olivetti, G., J. M. Capasso, E. H. Sonnenblick, and P. Anversa. 1990. Side-to-side slippage of myocytes participates in ventricular wall remodeling acutely after myocardial infarction in rats. *Circ. Res.* 67:23–34.

3. Ross, J., E. H. Sonnenblick, R. R. Taylor, H. M. Spotnitz, and J. W. Covell. 1971. Diastolic geometry and sarcomere length in the chronically dilated canine left ventricle. *Circ. Res.* 28:49–61.

4. Vitali-Mazza, L., P. Anversa, F. Tedeschi, R. Mastandrea, V. Mavilla, and O. Visioli. 1972. Ultrastructural basis of acute left ventricular failure from severe acute aortic stenosis in the rabbit. *J. Mol. Cell. Cardiol.* 4:661–671.

5. Kajstura, J., M. Mansukhani, W. Cheng, K. Reiss, S. Krajewski, J. C. Reed, F. Quaini, E. H. Sonnenblick, and P. Anversa. 1995. Programmed cell death and the expression of the protooncogene bcl-2 in myocytes during postnatal maturation of the heart. *Exp. Cell Res.* 219:110–121.

6. Hockenbery, D. M., Z. N. Olltvai, X. M. Yin, C. L. Milliman, and S. J. Korsmeyer. 1993. Bcl-2 functions in an antioxidant pathway to prevent apoptosis. *Cell.* 75:241–251.

7. Itoh, N., S. Yonehara, A. Ishii, M. Yonehara, S. Mizushima, M. Sameshima, A. Hase, Y. Seto, and S. Nagata. 1991. The polypeptide encoded by the cDNA for human cell surface antigen Fas can mediate apoptosis. *Cell.* 66:233–243.

8. Watanabe-Fukunaga, R., C. I. Brannan, N. J. Copeland, N. A. Jenkins, and S. Nagata. 1992. Lympho-proliferation disorder in mice explained by defects in Fas antigen that mediates apoptosis. *Nature (Lond).* 356:314–317.

9. Tanaka, M., H. Ito, S. Adachi, H. Akimoto, T. Nishikawa, T. Kasajima, F. Marumo, and M. Hiroe. 1994. Hypoxia induces apoptosis with enhanced expression of Fas antigen messenger RNA in cultured neonatal rat cardiomyocytes. *Circ. Res.* 75:426–433.

10. Mannick, J. B., K. Asano, K. Izumi, E. Kieff, and J. S. Stamler. 1994. Nitric oxide produced by human B lymphocytes inhibits apoptosis and Epstein-Barr virus reactivation. *Cell.* 79:1137–1146.

11. Furchgott, R. F., M. T. Khan, and K. D. Jothianandan. 1990. Comparison of properties of nitric oxide and endothelium-derived relaxing factor: some cautionary findings. *In* Endothelium-Derived Relaxing Factors, G. M. Rubanyi and P. M. Vanhoutte, editors. Karger, Basel. 8–21.

12. Niu, X.-F., C. W. Smith, and P. Kubes. 1994. Intracellular oxidative stress induced by nitric oxide synthesis inhibition increases endothelial cell adhesion to neutrophils. *Circ. Res.* 74:1133–1140.

13. Bohn, H., R. Beyerle, P. A. Martorana, and K. Schonafinger. 1991. CAS 936, a novel sydnonimine with direct vasodilating and nitric oxide-donating properties: effects on isolated blood vessels. *J. Cardiovasc. Pharmacol.* 18:522–527.

14. Li, P., E. H. Sonnenblick, P. Anversa, and J. M. Capasso. 1994. Length dependent modulation of angiotensin II inotropism in rat myocardium: effects of myocardial infarction. *Am. J. Physiol.* 266:H779–H786.

15. Gong, J., F. Traganos, and Z. Darzynkiewicz. 1994. A selective procedure for DNA extraction from apoptotic cells applicable for gel electrophoresis and flow cytometry. *Anal. Biochem.* 218:314–319.

16. Mohazzab, K. M., and M. S. Wolin. 1994. Properties of a superoxide anion generating microsomal NADH-oxidoreductase, a potential pulmonary artery PO_2 sensor. *Am. J. Physiol.* 267:L823–L831.

17. Bolli, R., M. O. Jeroudi, B. S. Patel, O. I. Aruoma, B. Halliwell, E. K. Lai, and P. B. McCay. 1989. Marked reduction of free radical generation and contractile dysfunction by antioxidant therapy begun at the time of reperfusion. *Circ. Res.* 65:607–622.

18. Kaminski, P. M., and M. S. Wolin. 1994. Hypoxia increases superoxide anion production from bovine coronary microvessels, but not cardiac myocytes, via increased xanthine oxidase. *Microcirculation.* 4:231–236.

19. Anversa, P., E. Puntillo, P. Nikitin, G. Olivetti, J. M. Capasso, and E. H. Sonnenblick. 1989. Effects of age on mechanical and structural properties of myocardium of Fischer 344 rats. *Am. J. Physiol.* 256:H1440–H1449.

20. Allen, D. G., and J. C. Kentish. 1985. The cellular basis of length-tension relation in cardiac muscle. *J. Mol. Cell. Cardiol.* 17:8281–840.

21. Gulati, J., E. H. Sonnenblick, and A. Babu. 1991. The role of TnC in the length dependence of Ca^{2+} sensitive force of mammalian skeletal and cardiac muscle. *J. Physiol.* 441:305–324.

22. Lakatta, E. G. 1986. Length modulation of muscle performance; Frank-Starling law of the heart. *In* The Heart and Cardiovascular System, Volume 2. H. A. Fozzard, E. Haber, R. B. Jennings, A. M. Katz, and H. E. Morgan, editors. Raven Press, Ltd., New York. 819–843.

23. Puceat, M., O. Clement, P. Lechene, J. M. Pelosin, R. Ventura-Clapier, and G. Vassort. 1991. Neuro-humoral control of calcium sensitivity of myofilaments in rat single heart cells. *Circ. Res.* 67:517–524.

24. Yoran, C., J. W. Covell, and J. Ross, Jr. 1973. Structural basis for the ascending limb of left ventricular function. *Circ. Res.* 32:297–303.

25. Anversa, P., P. Li, X. Zhang, G. Olivetti, and J. M. Capasso. 1993. Ischemic myocardial injury and ventricular remodeling. *Cardiovasc. Res.* 27:145–157.

26. Olivetti, G., J. M. Capasso, L. G. Meggs, E. H. Sonnenblick, and P. Anversa. 1991. Cellular basis of chronic ventricular remodeling after myocardial infarction in rats. *Circ. Res.* 68:856–869.

27. Gottlieb, R. A., K. O. Burleson, R. A. Kloner, B. M. Bablor, and R. L. Engler. 1994. Reperfusion injury induces apoptosis in rabbit cardiomyocytes. *J. Clin. Invest.* 94:1621–1628.

28. Darzynkiewicz, Z., S. Bruno, G. Del Bino, W. Gorczyca, M. A. Hotz, P. Lassota, and F. Traganos. 1992. Features of apoptotic cells measured by flow cytometry. *Cytometry.* 13:795–808.

29. Arends, M. J., R. G. Morris, and A. H. Wyllie. 1990. Apoptosis: the role of endonuclease. *Am. J. Pathol.* 136:593–608.

30. Majno, G., and I. Joris. 1995. Apoptosis, oncosis, and necrosis. An overview of cell death. *Am. J. Pathol.* 146:3–15.

31. McCord, J. M. 1985. Oxygen derived free radicals in post-ischemic tissue injury. *N. Engl. J. Med.* 312:159–163.

32. Turner, M. J., III, C. E. Fields, and D. B. Everman. 1991. Evidence for superoxide formation during hepatic metabolism of tamoxifen. *Biochem. Pharmacol.* 41:1701–1705.

33. Sugioka, K., M. Nakano, H. Totsune-Nakano, H. Minakami, S. Tero-Kubota, and Y. Ikegami. 1988. Mechanism of O_2 generation in reduction and oxidation cycle of ubiquinones in a model of mitochondrial electron transport systems. *Biochim. Biophys. Acta.* 936:377–385.

34. Sandstrom, P. A., M. D. Mannie, and T. M. Buttke. 1994. Inhibition of activation-induced death in T cell hybridomas by thiol antioxidants: oxidative stress as a mediator of apoptosis. *J. Leukocyte Biol.* 55:221–226.

35. Kanner, J., S. Harel, and R. Granit. 1992. Nitric oxide, an inhibitor of lipid oxidation by lipoxygenase, cyclooxygenase and hemoglobin. *Lipids.* 27:46–49.

36. Kiuchi, K., N. Sato, R. P. Shannon, D. E. Vatner, K. Morgan, and S. F. Vatner. 1993. Depressed β-adrenergic receptor- and endothelium-mediated vasodilation in conscious dogs with heart failure. *Circ. Res.* 73:1013–1023.

37. Shen, W., X. Xu, M. Ochoa, G. Zhao, M. S. Wolin, and T. H. Hintze. 1994. Role of nitric oxide in the regulation of oxygen consumption in conscious dogs. *Circ. Res.* 75:1086–1095.

38. Hare, J. M., J. F. Keaney, Jr., J. L. Balligand, J. Loscalzo, T. W. Smith, and W. S. Colucci. 1995. Role of nitric oxide in parasympathetic modulation of β-adrenergic myocardial contractility in normal dogs. *J. Clin. Invest.* 95:360–366.

39. Balligand, J. L., D. Ungureanu, R. A. Kelly, and T. Smith. 1993. Abnormal contractile function due to induction of nitric oxide synthesis in rat cardiac myocytes follows exposure to activated macrophage conditioned medium. *J. Clin. Invest.* 91:2314–2319.

40. Brady, A. J. B., P. A. Poole-Wilson, S. E. Harding, and T. Pickering. 1993. Nitric oxide production within cardiac myocytes reduced their contractility in endotoxemia. *Am. J. Physiol.* 265:H176–H182.